

Angiotensin II activates two cation conductances with distinct TRPC1 and TRPC6 channel properties in rabbit mesenteric artery myocytes

S. N. Saleh, A. P. Albert, C. M. Peppiatt and W. A. Large

Ion Channels and Cell Signalling, Division of Basic Medical Sciences, St George's, University of London, London SW17 0RE, UK

Angiotensin II (Ang II) is a potent vasoconstrictor with an important role in controlling blood pressure; however, there is little information on cellular mechanisms underlying Ang II-evoked vasoconstrictor responses. The aim of the present study is to investigate the effect of Ang II on cation conductances in freshly dispersed rabbit mesenteric artery myocytes at the single-channel level using patch-clamp techniques. In cell-attached patches, bath application of low concentrations of Ang II (1 nM) activated cation channel currents (I_{cat1}) with conductance states of about 15, 30 and 45 pS. At relatively high concentrations, Ang II (100 nM) inhibited I_{cat1} but evoked another cation channel (I_{cat2}) with a conductance of approximately 2 pS. Ang II-evoked I_{cat1} and I_{cat2} were inhibited by the AT_1 receptor antagonist losartan and the phospholipase C (PLC) inhibitor U73122. The diacylglycerol (DAG) lipase inhibitor RHC80267 initially induced I_{cat1} which was subsequently inhibited to reveal I_{cat2} . The DAG analogue 1-oleoyl-2-acetyl-*sn*-glycerol (1 μM) activated I_{cat1} and I_{cat2} but inositol 1,4,5-trisphosphate did not evoke either conductance. The protein kinase C (PKC) inhibitor chelerythrine (3 μM) potentiated Ang II-evoked I_{cat1} and inhibited I_{cat2} whereas the PKC activator phorbol-12,13-dibutyrate (1 μM) reduced Ang II-induced I_{cat1} but activated I_{cat2} . Moreover in cell-attached patches pretreated with chelerythrine, application of 100 nM Ang II activated I_{cat1} . These data indicate that PKC inhibits I_{cat1} but stimulates I_{cat2} . Agents that deplete intracellular Ca^{2+} stores also activated cation channel currents with similar properties to I_{cat2} . Bath application of anti-TRPC6 and anti-TRPC1 antibodies to inside-out patches inhibited I_{cat1} and I_{cat2} , respectively. Also flufenamic acid and zero external Ca^{2+} concentration, respectively, potentiated and reduced Ang II-evoked I_{cat1} . Immunocytochemical studies showed TRPC6 and TRPC1 expression with TRPC6 preferentially distributed in the plasma membrane and TRPC1 expression located throughout the myocyte. These results indicate that Ang II activates two distinct cation conductances in mesenteric artery myocytes by stimulation of AT_1 receptors linked to PLC. I_{cat1} is activated by DAG via a PKC-independent mechanism whereas I_{cat2} involves DAG acting via a PKC-dependent pathway. Higher concentrations of Ang II inhibit I_{cat1} by activating an inhibitory effect of PKC. It is proposed that TRPC6 and TRPC1 channel proteins are important components of Ang II-induced I_{cat1} and I_{cat2} , respectively.

(Resubmitted 16 August 2006; accepted after revision 12 September 2006; first published online 14 September 2006)

Corresponding author A. P. Albert: Ion Channels and Cell Signalling, Division of Basic Medical Sciences, St George's, University of London, Cranmer Terrace, London SW17 0RE, UK. Email: aalbert@sgul.ac.uk

OnlineOpen: This article is available free online at www.blackwell-synergy.com

Angiotensin II (Ang II) is an endogenous octapeptide that has important actions in the cardiovascular system including regulation of blood pressure and plasma volume. Ang II is a potent vasoconstrictor that produces direct contraction of vascular smooth muscle via AT_1

receptors and hence regulates total peripheral resistance. Clinically, antagonists of Ang II receptors are used in various diseases such as essential hypertension and cardiac failure but despite its importance little is known about the cellular mechanisms underlying the vasoconstrictor responses to Ang II.

In vascular smooth muscle the primary trigger for agonist-induced contraction is a rise in intracellular Ca^{2+} concentration ($[\text{Ca}^{2+}]_i$) which is achieved by release

Re-use of this article is permitted in accordance with the Creative Commons Deeds, Attribution 2.5, which does not permit commercial exploitation.

of Ca^{2+} ions from the sarcoplasmic reticulum (SR) and by influx of Ca^{2+} ions through both classical voltage-dependent Ca^{2+} channels (VDCCs) and also voltage-independent pathways (see Large, 2002). Ang II appears to conform to these principles as it causes a biphasic $[\text{Ca}^{2+}]_i$ signal consisting of an immediate rapid rise due to inositol 1,4,5-trisphosphate (IP_3)-mediated release of Ca^{2+} from the SR followed by a sustained influx of Ca^{2+} ions (see review by Touyz & Schiffrin 2000). It is evident that a major component of Ca^{2+} influx caused by Ang II is resistant to antagonists of L-type VDCCs indicating that voltage-independent Ca^{2+} -permeable non-selective cation channels are activated by Ang II to produce Ca^{2+} influx (Touyz & Schiffrin, 2000). In agreement with this hypothesis, there has been a brief report showing that Ang II activates a non-selective cation current in rabbit ear artery myocytes (Hughes & Bolton, 1995) but no information was provided on the unitary properties or molecular identity of the underlying ion channels.

Members of the transient receptor potential (TRP) channel proteins form non-selective cation channels which can be activated by depletion of intracellular Ca^{2+} stores (store-operated channels, SOCs) or by pharmacological receptor stimulation (receptor-operated channels, ROCs, Clapham, 2003). There is accumulating evidence that the canonical subgroup of TRP channel proteins (TRPC channels) are widely distributed in smooth muscle and have important functions in vascular smooth muscle (for reviews see Large, 2002; Beech *et al.* 2004; Albert & Large, 2006). With respect to ROCs, it has been shown that noradrenaline activates TRPC6 in rabbit portal vein (Inoue *et al.* 2001) but TRPC3 is stimulated by this neurotransmitter in rabbit ear artery (Albert *et al.* 2003, 2006). Evidence has also been provided that TRPC3 channels mediate pyrimidine-induced depolarization in cerebral arteries (Reading *et al.* 2005). With these limited data, there are no clear patterns regarding specific cation channels activated by vasoconstrictor agents in vascular smooth muscle.

In the present work, we have studied the biophysical properties of single cation channels activated by Ang II in freshly dispersed rabbit mesenteric artery myocytes. Moreover, the transduction mechanisms linking the pharmacological receptor to the channels and the possibility that TRPC channel proteins may form these channels have been investigated. It is shown that Ang II activates two distinct cation channels, with different gating mechanisms, that have TRPC1 and TRPC6 properties.

Methods

Cell isolation

New Zealand White rabbits (2–3 kg) were killed by an i.v. injection of sodium pentobarbitone (120 mg kg^{-1}), in

accordance with the UK Animals (Scientific Procedures) Act, 1986, and sections of mesenteric artery were removed (second to fifth order). Mesentery arteries were then cleaned and endothelium removed with cotton buds and dispersed using enzymatic procedures and solutions previously described (Albert *et al.* 2003).

Electrophysiology

Whole-cell and single cation channel currents were recorded with an Axopatch 200B patch-clamp amplifier (Axon Instruments, Union City, CA, USA) at room temperature ($20\text{--}23^\circ\text{C}$) using whole-cell recording, cell-attached, inside-out and outside-out patch configurations of the patch-clamp technique (Hamill *et al.* 1981). Patch pipettes were manufactured from borosilicate glass and then fire polished to produce pipettes with resistances of about $6 \text{ M}\Omega$ for whole-cell and $10 \text{ M}\Omega$ for isolated patch recording when filled with patch pipette solution. To reduce 'line' noise, the recording chamber (volume, $\sim 150\text{--}200 \mu\text{l}$) was perfused using two 20 ml syringes, one filled with external solution and the other used to drain the chamber, in a 'push and pull' technique. The external solution could be exchanged twice within 30 s. Whole-cell current–voltage ($I\text{--}V$) relationships were evoked by applying voltage ramps from -100 to $+100 \text{ mV}$ (0.5 V s^{-1}) every 20 s from a holding potential of -50 mV and filtered at 1 kHz (Axopatch 200B patch-clamp amplifier) and sampled at 10 kHz (Digidata 1322A and pCLAMP 9.0, Axon Instruments). Experiments were only continued if the control whole-cell currents were stable. When recording single-channel currents, the holding potential was routinely set between -70 and -50 mV and to evaluate $I\text{--}V$ characteristics of single-channel currents the membrane potential was manually changed between -120 and $+50 \text{ mV}$.

Single-channel currents were initially recorded onto digital audiotape (DAT) using a Biologic DRA-200 digital tape recorder (BioLogic Science Instruments, France) at a bandwidth of 5 kHz (Axopatch 200B patch-clamp amplifier) and a sample rate of 48 kHz. For off-line analysis, single cation channel records were filtered at either 100 Hz or 1 kHz (see below, -3 dB , low pass 8-pole Bessel filter, Frequency Devices, model LP02, Scensys Ltd, Aylesbury, UK) and acquired using a Digidata 1322A and pCLAMP 9.0 at sampling rates of 1 and 10 kHz, respectively. The level of filtering depended on the amplitude of channel currents analysed with I_{cat1} channel currents (see later for definition) filtered at 1 kHz and I_{cat2} channel currents at 100 Hz. Data were captured with a Pentium III personal computer (Research Machines).

Single-channel current amplitudes were calculated from idealized traces of at least 10 s in duration using the 50% threshold method with events lasting for $< 0.664 \text{ ms}$ and $< 6.664 \text{ ms}$ ($2 \times$ rise time for a 1 kHz and 100 Hz (-3 dB)).

low-pass filter) being excluded from analysis (Colquhoun, 1987). Figure preparation was carried out using MicroCal Origin software 6.0 (MicroCal Software Inc., MA, USA) where inward channel currents are shown as downward deflections. The number of channels in a patch was unknown and therefore open probability (NP_o) was calculated using the equation: $NP_o = \text{total open time of all channel levels in the patch/sample duration}$.

Immunocytochemistry

Freshly dispersed myocytes were fixed with either 4% paraformaldehyde in physiological saline solution (PSS, see Albert *et al.* 2003) or 70% ethanol in PBS (Sigma, UK) for 10 min at room temperature and then washed with PBS and permeabilized with PBS containing 0.5% Triton X-100 for 20 min at room temperature. After cells were incubated with PBS containing 10% chicken serum and 0.1% Triton X-100 for 1 h at room temperature, the cells were then incubated with anti-TRPC antibodies (1 : 50 dilution) in PBS containing 10% chicken serum overnight at 4°C. The cells were then washed and incubated with secondary antibodies conjugated to a fluorescent probe (Alexa Fluor 488-conjugated chicken anti-rabbit antibody, 1 : 200). In control experiments, the primary antibodies were preincubated for 12 h at 4°C with antigenic peptide (1 : 25). After removing the unbound secondary antibodies by washing the preparations with PBS the myocytes were imaged using laser scanning confocal microscope.

Confocal microscopy

The cells were imaged using a Zeiss LSM 510 laser scanning confocal microscope (Carl Zeiss, Jena, Germany). The excitation beam was produced by an argon laser (488 nm) and delivered to the specimen via a Zeiss Apochromat $\times 63$ oil immersion objective (numerical aperture, 1.4). Emitted fluorescence was captured using LSM 510 software (release 3.2, Carl Zeiss, Jena, Germany). A two-dimensional image of the cells, cutting horizontally through approximately the middle of the cell, was captured (1024 \times 1024 pixels).

Raw confocal imaging data were processed and analysed using Zeiss LSM 510 software. To assess the cellular distribution of TRPC channel proteins, a circular area of 0.78 μm^2 (diameter about 1 μm and referred to as Region 1) was randomly selected in the subplasmalemmal area of the cell so that its perimeter touched the edge of the cell from the inside. Another circular area of 0.78 μm^2 (Region 2) was selected so that the perimeter of such a circle touched the perimeter of Region 1 and the line going through centres of these circles was perpendicular to the edge of the cell, thought to be the plasma membrane. A percentage of fluorescing pixels (%FP) were calculated in

both regions using the formula:

$$\%FP = 100 \times \frac{n(p > \text{threshold})}{n(p)}$$

where $n(p > \text{threshold})$ is the number of pixels within the region whose intensity equalled or exceeded the threshold value (one standard deviation, to exclude low intensity pixels caused by photomultiplier noise) and $n(p)$ the total number of pixels in the region. The %FP values were then compared with each other and with the %FP in the whole confocal plane of the cell. The average pixel fluorescence (APF) value was used to compare the overall fluorescence signal between the staining and its controls and was calculated using the formula:

$$APF = \frac{\sum i(p)}{n(p)} (\text{I.U./pixel})$$

Where $i(p)$ is the intensity of a pixel within the confocal plane of the cell and $n(p)$ is the total number of pixels of the plane. Statistical evaluation and graphs were created using Origin and final images were produced using Microsoft PowerPoint.

Solutions and drugs

The bathing solution used in whole-cell recording experiments was K^+ -free and contained (mM): NaCl 126, CaCl_2 1.5, Hepes 10, glucose 11, 4,4'-diisothiocyanatostilbene-2,2'-disulfonic acid (DIDS) 0.1, niflumic acid 0.1 and nicardipine 0.005; pH adjusted to 7.2 with NaOH. The pipette solution used for whole-cell recording was also K^+ -free and contained (mM): CsCl 18, caesium aspartate 108, MgCl 1.2, Hepes 10, glucose 11, EGTA 1, CaCl_2 0.3 (free internal Ca^{2+} concentration approximately 80 nM as calculated using EQCAL software), Na_2ATP 1, NaGTP 0.2; pH adjusted to 7.2 with Tris. In cell-attached patch experiments the membrane potential was set to approximately 0 mV by perfusing cells in a KCl-containing solution containing (mM): KCl 126, CaCl_2 1.5, Hepes 10 and glucose 11; pH adjusted to 7.2 with 10 M NaOH. Nicardipine (5 μM) was also included to prevent smooth muscle cell contraction by blocking Ca^{2+} entry through VDCCs. The composition of the bathing solution used in inside-out experiments (intracellular solution) was the same as the pipette solution used for whole-cell recording except that 1 mM BAPTA and 0.48 mM CaCl_2 were included (free internal Ca^{2+} concentration approximately 100 nM). The pipette solution used for both cell-attached and inside-out recording (extracellular solution) was K^+ -free and contained (mM): NaCl 126, CaCl_2 1.5, Hepes 10, glucose 11, TEA 10, 4-aminopyridine 5, iberiotoxin 0.0002, DIDS 0.1, niflumic acid 0.1 and nicardipine 0.005; pH adjusted to 7.2 with NaOH. Under these conditions, VDCCs, K^+ currents, swell-activated Cl^- currents and Ca^{2+} -activated

conductances are abolished and non-selective cation currents can be recorded in isolation.

All drugs were purchased from Sigma (UK) except for RHC80267 (Biomol, UK) and losartan (VWR, UK). Agents were dissolved in distilled H₂O or DMSO and 0.1% solution of DMSO alone had no effect on whole-cell or single-channel currents. In the Ca²⁺-free external solution (0[Ca²⁺]_o), CaCl₂ was removed and 1 mM BAPTA was added (< 10 nM free Ca²⁺ concentration). Anti-TRPC antibodies raised against putative intracellular epitopes were obtained from Alomone Laboratories (Israel; TRPC1, C3, C6, defined as TRPCa) and Santa Cruz Biotechnology (CA, USA; TRPC1, C3, C6, C7, defined as TRPCsc). The values are the mean ± s.e.m. of *n* cells. Statistical analysis was carried out using paired (comparing effects of agents on the same cell) or unpaired (comparing effects of agents between cells) Student's *t* test with the level of significance set at *P* < 0.05.

Results

Effect of Ang II on whole-cell currents in rabbit mesenteric artery myocytes

We initially investigated the effect of Ang II on macroscopic cation conductances in mesenteric artery myocytes using the whole-cell recording configuration of the patch-clamp technique. At a holding potential of -50 mV, bath application of 1–100 nM Ang II activated a 'noisy' inward current with a mean peak amplitude of -46 ± 21 pA which exhibited *I*-*V* relationships with a mean reversal potential (*E*_r) of $+3 \pm 2$ mV (*n* = 14). As the chloride equilibrium potential is about -45 mV and the bath solution contained several Cl⁻ channel blockers and was K⁺-free (see Methods), it is evident that Ang II activates a non-selective cation conductance in rabbit mesenteric artery myocytes.

We recorded single-channel activity in response to bath applied Ang II using the cell-attached configuration of the patch-clamp technique in order to obtain more precise information about the ionic conductance(s) involved.

Ang II activates two distinct cation channels in cell-attached patches

Figure 1A shows a typical response of cation channel currents induced by increasing concentrations of Ang II in a cell-attached patch held at -70 mV. Bath application of 1 nM Ang II activated cation channel currents which opened to multiple unitary current amplitude levels producing a characteristic 'noisy' appearance (Fig. 1Aa). We termed these channel currents *I*_{cat1} and in 11 patches 1 nM Ang II induced *I*_{cat1} activity with a mean peak *NP*_o value of 0.264 ± 0.112 at -70 mV. In all patches tested, 1 nM Ang II-evoked *I*_{cat1} displayed discrete transitions

between three unitary amplitudes and Fig. 1Bb illustrates that the amplitude histogram of *I*_{cat1} activity shown in Fig. 1A could be described by four Gaussian curves with peaks representing a closed level and three open levels. Figure 1Ca shows the mean pooled *I*-*V* relationships of the three unitary amplitudes activated by 1 nM Ang II and illustrates that these three levels had conductance states of 15, 29 and 44 pS which all had a similar *E*_r of about 0 mV. The observations that in all patches tested *I*_{cat1} consisted of three current levels and no patch contained one or two levels, that discrete transitions occurred between these three levels and that all three states had a similar *E*_r may suggest that *I*_{cat1} consists of a single channel with three subconductance states. However, as the second and third levels were close multiple of the lower level it is possible that all patches tested contained at least three *I*_{cat1} channels and the different levels represented multiple openings.

Figure 1A also shows a typical response of increasing the concentration of Ang II from 1 to 100 nM which completely blocked activation of *I*_{cat1}. Instead, single-channel currents with much smaller unitary amplitudes of about -0.2 pA at -70 mV (Fig. 1Ab) were recorded in the presence of 100 nM Ang II. These channel currents were termed *I*_{cat2} and in 11 patches *I*_{cat2} activity evoked by 100 nM Ang II had a mean *NP*_o of 0.392 ± 0.153 at -70 mV. Figure 1Bb illustrates that the amplitude histogram of *I*_{cat2} shown in Fig. 1A after application of 100 nM Ang II could be fitted by three Gaussian curves with peaks representing a closed level, an unitary open level and another level reflecting more than one *I*_{cat2} channel in the patch. Figure 1Cb shows the mean pooled *I*-*V* relationship of *I*_{cat2} present in 100 nM Ang II had a slope conductance between -120 and -50 mV of 2.1 pS with an extrapolated *E*_r of about +23 mV; these values are significantly different from the conductance and *E*_r values of *I*_{cat1} described above (*P* < 0.001). It should be noted that because the activity of *I*_{cat1} evoked by 1 nM Ang II was relatively high and the unitary amplitude of *I*_{cat2} is small, we were unable to accurately determine whether *I*_{cat2} was activated by 1 nM Ang II.

These data clearly show that Ang II activates two cation channel conductances with distinct single-channel properties in mesenteric artery myocytes and importantly our results indicate that *I*_{cat1} is activated by low concentrations (1 nM) of Ang II whereas at relatively high concentrations (100 nM) of Ang II a second ion channel, *I*_{cat2}, is evoked.

Ang II activates *I*_{cat1} and *I*_{cat2} through stimulation of AT₁ receptors and U73122-sensitive phospholipase C in cell-attached patches

It is well established that Ang II-induced vasoconstriction is associated with stimulation of the AT₁ subtype of G-protein-coupled receptors linked to activation of

phospholipase C (PLC, Touyz & Schiffrin, 2000) and in the next series of experiments we investigated the role of this signalling pathway in activating I_{cat1} and I_{cat2} by 1 nM and 100 nM Ang II, respectively.

Figure 2A shows that in the presence of the selective AT_1 receptor antagonist losartan ($1 \mu M$), 1 nM Ang II evoked only a very small activation of I_{cat1} ; however, I_{cat1} activity was markedly increased following washout of losartan. In the presence of $1 \mu M$ losartan, bath application of 1 nM Ang II activated I_{cat1} activity with a mean NP_o value of 0.051 ± 0.034 which was significantly increased to 0.362 ± 0.122 at -50 mV ($n = 7, P < 0.05$) following

washout of losartan. Figure 2B also shows that preincubation with $1 \mu M$ losartan had a similar effect on I_{cat2} activity evoked by 100 nM Ang II and in seven patches; the mean NP_o of I_{cat2} evoked by 100 nM Ang II was significantly increased from 0.009 ± 0.005 to 0.197 ± 0.081 ($P < 0.05$) at -70 mV following washout of losartan. These data indicate that both I_{cat1} and I_{cat2} are mediated by AT_1 receptors.

Figure 2C and D shows that co-application $2 \mu M$ U73122, a PLC inhibitor, reduced I_{cat1} and I_{cat2} activity induced by 1 nM and 100 nM Ang II, respectively, with mean NP_o values of I_{cat1} activity significantly reduced by

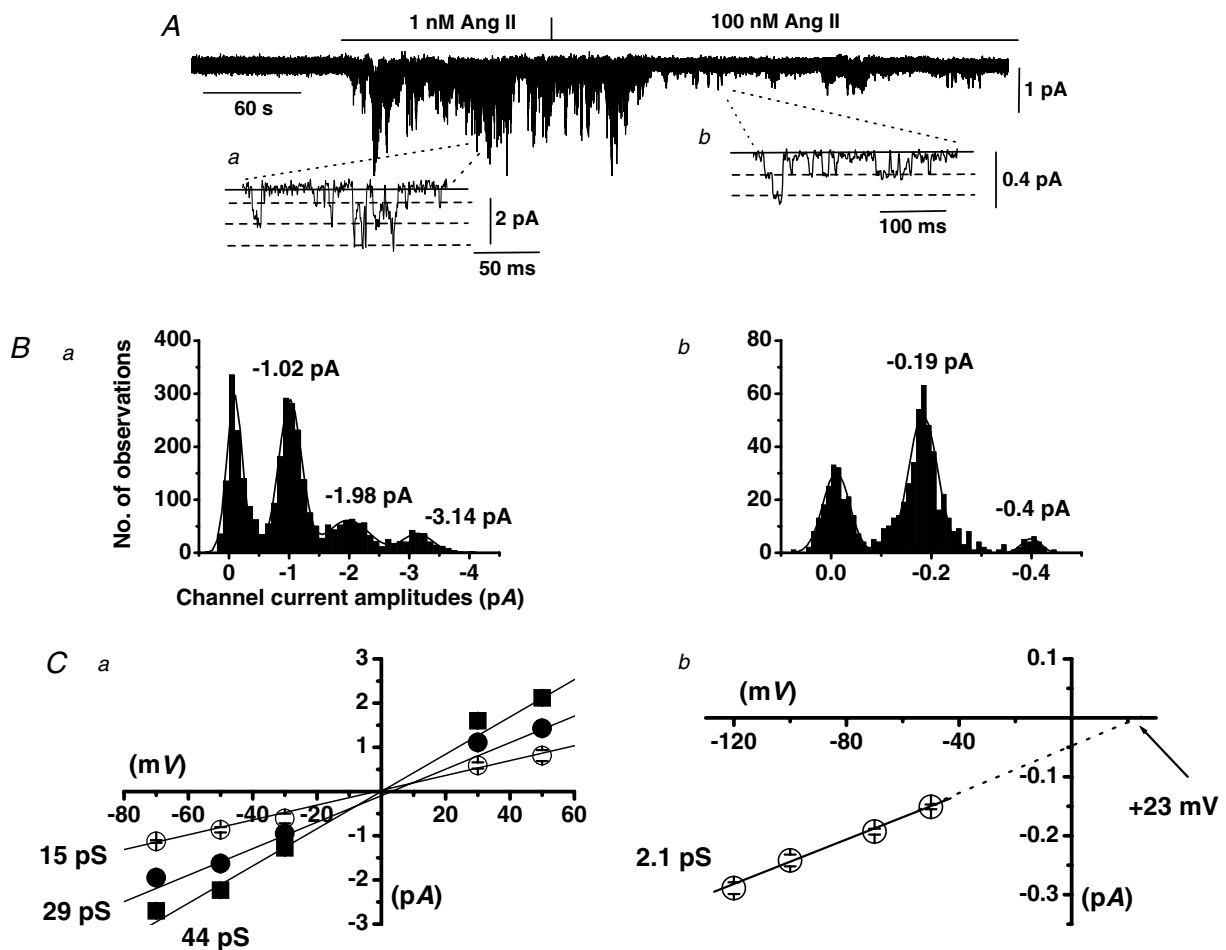


Figure 1. Ang II activates two distinct cation channels in cell-attached patches from mesenteric artery myocytes

A, shows that bath application of 1 nM Ang II activated cation channel currents which had three amplitude levels at -70 mV (see inset a). In the presence of 100 nM Ang II, this conductance was not present but channel currents with a smaller unitary amplitude of about -0.2 pA at -70 mV were revealed (see inset b). B, amplitude histograms of cation channel currents recorded in 1 nM (a) and 100 nM (b) Ang II. Channel currents evoked by 1 nM Ang could be fitted with four Gaussian curves representing one closed and three amplitude levels whereas the channel currents present in 100 nM Ang II could be fitted by three Gaussians representing a closed and an open level with the largest Gaussian representing more than one channel in the patch. C, shows the mean pooled $I-V$ relationship of cation channel currents evoked by 1 nM Ang II which had three conductance states of 15, 29 and 44 pS and all had an E_r of about $+5$ mV (a), and the mean pooled $I-V$ relationship of cation channel currents present in 100 nM Ang II which had a unitary conductance of 2.1 pS and an extrapolated E_r of $+18$ mV (b).

$95 \pm 2\%$ ($n = 7$, $P < 0.001$) and $I_{\text{cat}2}$ activity significantly inhibited by $77 \pm 9\%$ ($n = 7$, $P < 0.05$). In control experiments, $2 \mu\text{M}$ U73433, an inactive analogue of U73122, had no effect on Ang II-evoked $I_{\text{cat}1}$ ($n = 5$) or $I_{\text{cat}2}$ activity ($n = 6$).

Activation of $I_{\text{cat}1}$ and $I_{\text{cat}2}$ by endogenous diacylglycerol and by the analogue 1-oleoyl-2-acetyl-*sn*-glycerol

The above results indicate that Ang II evokes both $I_{\text{cat}1}$ and $I_{\text{cat}2}$ by acting on AT_1 receptors linked to activation of a U73122-sensitive PLC, and stimulation of this phospholipase hydrolyses phosphatidylinositol 4,5-bisphosphate (PIP_2) to produce the second messengers diacylglycerol (DAG) and IP_3 . Therefore in the next series of experiments we investigated the role of these two products of PLC activation in mediating activation of $I_{\text{cat}1}$ and $I_{\text{cat}2}$.

Figure 3A shows a typical effect of the DAG lipase inhibitor, RHC80267, on $I_{\text{cat}1}$ and $I_{\text{cat}2}$ activity in a cell-attached patch held at -70 mV. This agent prevents the breakdown of endogenous DAG production into arachidonic acid and therefore it is predicted that RHC80267 will induce an increase in the levels of endogenous DAG if this metabolic pathway is constitutively active. Bath application of $10 \mu\text{M}$ RHC80267 initially activated $I_{\text{cat}1}$ and subsequently $I_{\text{cat}1}$ was inhibited and $I_{\text{cat}2}$

was recorded (Fig. 3A). In nine patches, $10 \mu\text{M}$ RHC80267 induced $I_{\text{cat}1}$ activity with a mean peak NP_o value of 0.193 ± 0.041 which after 5 min was abolished to reveal $I_{\text{cat}2}$ activity with a mean NP_o value of 0.218 ± 0.073 .

These data show that RHC80267 mimics the effect of increasing Ang II concentration in evoking $I_{\text{cat}1}$ and $I_{\text{cat}2}$ which suggests that endogenous DAG has an important role in mediating the activation of both these cation channels.

Figure 3B shows that bath application of the membrane-permeable DAG analogue 1-oleoyl-2-acetyl-*sn*-glycerol (OAG, $1 \mu\text{M}$) activated cation channel currents in a cell-attached patch held at -70 mV which had unitary amplitudes of about -0.2 pA. In five patches, $1 \mu\text{M}$ OAG induced channel activity with a mean NP_o value of 0.261 ± 0.016 and the mean pooled $I-V$ relationship showed that these channel currents had a slope conductance between -120 and -50 mV of 1.9 pS with an extrapolated E_r of $+16$ mV. These results indicate the OAG activates $I_{\text{cat}2}$ in cell-attached patches which further suggests that DAG has a role in mediating $I_{\text{cat}2}$ activity in mesenteric artery myocytes.

In all cell-attached patches tested ($n = 15$), bath application of 1 nM to $100 \mu\text{M}$ OAG did not activate $I_{\text{cat}1}$ activity but Fig. 3C shows that bath application of $1 \mu\text{M}$ OAG to the cytoplasmic surface of an inside-out patch held at -50 mV did evoke $I_{\text{cat}1}$. In nine inside-out patches, $1 \mu\text{M}$ OAG induced channel activity which had a mean NP_o value

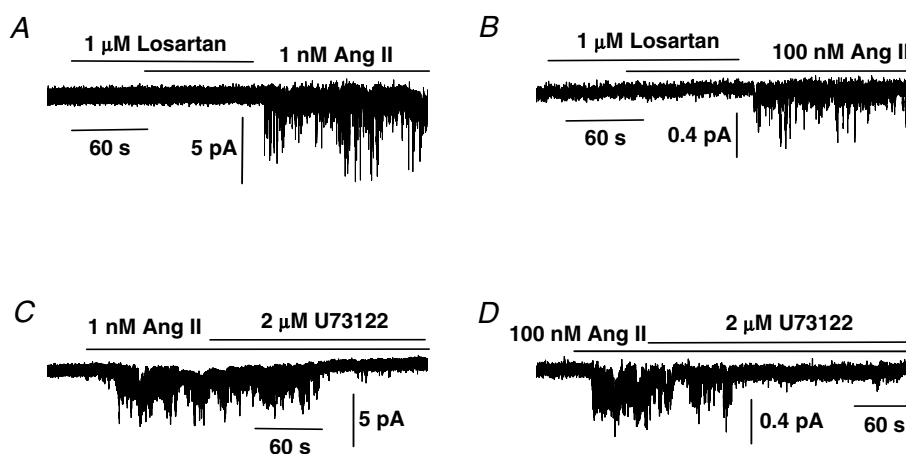


Figure 2. Effect of the AT_1 receptor antagonist losartan and the PLC inhibitor U73122 on $I_{\text{cat}1}$ and $I_{\text{cat}2}$ in cell-attached patches

A, shows that preincubation of $1 \mu\text{M}$ losartan prevented 1 nM Ang II from activating $I_{\text{cat}1}$ at -50 mV but that following washout of losartan Ang II-activated $I_{\text{cat}1}$ was evoked. B, shows that preincubation with $1 \mu\text{M}$ losartan also prevented activation of $I_{\text{cat}2}$ by 100 nM Ang II at -70 mV but that $I_{\text{cat}2}$ activity was stimulated upon washout of losartan. C and D, shows that co-application of $2 \mu\text{M}$ U73122 inhibited activation of $I_{\text{cat}1}$ (at -50 mV) and $I_{\text{cat}2}$ (at -70 mV) by, respectively, 1 nM and 100 nM Ang II in two different cell-attached patches.

of 0.930 ± 0.335 and the mean pooled $I-V$ relationship of these channel currents had three conductance states of 13, 25 and 43 pS with an E_r between 0 and +5 mV. These values are identical to those of I_{cat1} stimulated by 1 nM Ang II and therefore it appears that DAG activates both ion conductances.

We also investigated the effect of IP_3 on I_{cat1} and I_{cat2} activity and found that bath application of $10 \mu M$ IP_3 to the cytoplasmic surface of inside-out patches held at -70 mV did not induce any channel activity in 12 patches tested. In a previous study, we showed that IP_3 potentiated OAG-evoked TRPC6-like channel activity in rabbit portal vein myocytes (Albert & Large, 2003) and therefore we tested the effect of IP_3 on OAG-mediated I_{cat1} activity in inside-out patches. In five patches, bath application of $10 \mu M$ IP_3 did not increase the activity of I_{cat1} evoked by $1 \mu M$ OAG (data not shown). These results clearly indicate that IP_3 is not involved in directly activating I_{cat1} or I_{cat2} .

Effect of the protein kinase C inhibitor, chelerythrine, and phorbol-12,13-dibutyrate, a PKC activator, on Ang II-activated I_{cat1} and I_{cat2} activity in cell-attached patches

Production of DAG leads to stimulation of protein kinase C (PKC) which is implicated in many cellular processes involving phosphorylation of serine/threonine residues

within proteins, including ion channel proteins. Therefore, we investigated the role of PKC in regulating Ang II-evoked I_{cat1} and I_{cat2} activity by investigating the effect of agents that inhibit and activate PKC on these channel currents.

Figure 4A shows that bath application of the PKC inhibitor chelerythrine ($3 \mu M$) increased the activity of I_{cat1} induced by 1 nM Ang II and in six patches the mean NP_o value of Ang II-evoked I_{cat1} activity was increased by 4.6 ± 0.1 -fold ($P < 0.05$) in the presence of chelerythrine. In contrast, Fig. 4B illustrates that co-application of $3 \mu M$ chelerythrine inhibited I_{cat2} activity evoked by 100 nM Ang II and in 10 patches; the mean NP_o value of Ang II-evoked I_{cat2} activity was reduced by $87 \pm 5\%$ ($P < 0.05$). Application of the PKC activator phorbol-12,13-dibutyrate (PDBu, $1 \mu M$) suppressed I_{cat1} activity evoked by 1 nM Ang II by $51 \pm 6\%$ ($n = 6, P < 0.05$, Fig. 4C) whereas application of $1 \mu M$ PDBu to quiescent cell-attached patches activated channel currents which had a unitary amplitude of about -0.2 pA and a mean NP_o value of 0.334 ± 0.116 at -70 mV ($n = 5$, Fig. 4D). The mean pooled $I-V$ relationship of these PDBu-evoked channel currents had a slope conductance between -120 and -50 mV of 2 pS and an extrapolated E_r of +20 mV (data not shown), and hence phorbol esters stimulate I_{cat2} .

These data provide strong evidence that Ang II-evoked PKC stimulation has opposing actions on I_{cat1} and I_{cat2} activity with an inhibitory effect on I_{cat1} and a pivotal role in evoking I_{cat2} . These effects of PKC on I_{cat1} and

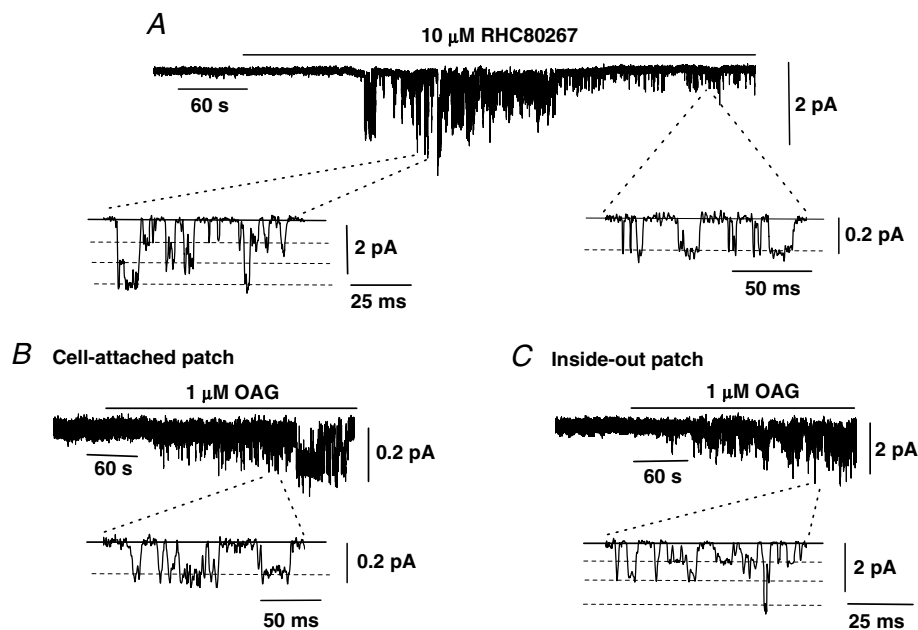


Figure 3. Effect of the diacylglycerol (DAG) lipase inhibitor RHC80267 and the DAG analogue 1-oleoyl-2-acetyl-*sn*-glycerol (OAG) on I_{cat1} and I_{cat2}

A, bath application of $10 \mu M$ RHC80267 evoked a transient activation of I_{cat1} and subsequently only I_{cat2} was recorded in a cell-attached patch held at -70 mV. B, illustrates that bath application of $1 \mu M$ OAG activated I_{cat2} in a cell-attached patch held at -70 mV. C, shows that bath application of $1 \mu M$ OAG evoked I_{cat1} in an inside-out patch held at -50 mV.

$I_{\text{cat}2}$ activity combined with the data implicating DAG in activating both these channels (Fig. 3, see above), suggests that Ang II activates $I_{\text{cat}1}$ through production of DAG which opens channels via a PKC-independent mechanism whereas Ang II evokes $I_{\text{cat}2}$ through DAG acting via a PKC-dependent pathway.

We described earlier that in cell-attached patches 100 nM Ang II and OAG only evoked $I_{\text{cat}2}$ and did not activate $I_{\text{cat}1}$. As a result of the above data on the inhibitory action of PKC on $I_{\text{cat}1}$ activity, we hypothesized that the failure of these agents to activate $I_{\text{cat}1}$ may be due to their ability to stimulate PKC activity and hence inhibit $I_{\text{cat}1}$. Therefore we investigated the effect of pretreating myocytes with the PKC inhibitor chelerythrine before applying 100 nM Ang II and 1 μM OAG.

Figure 4E and F shows that following pretreatment with 3 μM chelerythrine for at least 2 min, co-application of 100 nM Ang II and 1 μM OAG stimulated $I_{\text{cat}1}$ activity with mean NP_0 values of 1.874 ± 0.373 ($n = 8$) and 0.184 ± 0.049 ($n = 6$), respectively. The mean pooled $I-V$ relationships of $I_{\text{cat}1}$ evoked by 100 nM Ang II and 1 μM OAG in the presence of chelerythrine had similar

conductance states and E_r as those values described earlier for $I_{\text{cat}1}$ activity (Fig. 1).

These results indicate that Ang II at relatively high concentrations does not activate $I_{\text{cat}1}$ as a result of stimulation of PKC which has a potent inhibitory effect on $I_{\text{cat}1}$ activity. Of importance, these data also show that even relatively low concentrations of OAG (< 1 μM) do not activate $I_{\text{cat}1}$ because of its ability to stimulate PKC activity. Moreover these data provide conclusive evidence that $I_{\text{cat}1}$ is evoked by DAG activity via a PKC-independent mechanism and is inhibited by PKC stimulation.

Activation of $I_{\text{cat}2}$ activity by agents that are proposed to deplete intracellular Ca^{2+} stores

We have previously described in rabbit portal vein myocytes a cation channel evoked by agents that deplete intracellular Ca^{2+} stores which had similar properties to Ang II-evoked $I_{\text{cat}2}$ described in the present work (Albert & Large, 2002a,b). Therefore, to further investigate the similarity between these two cation channel currents

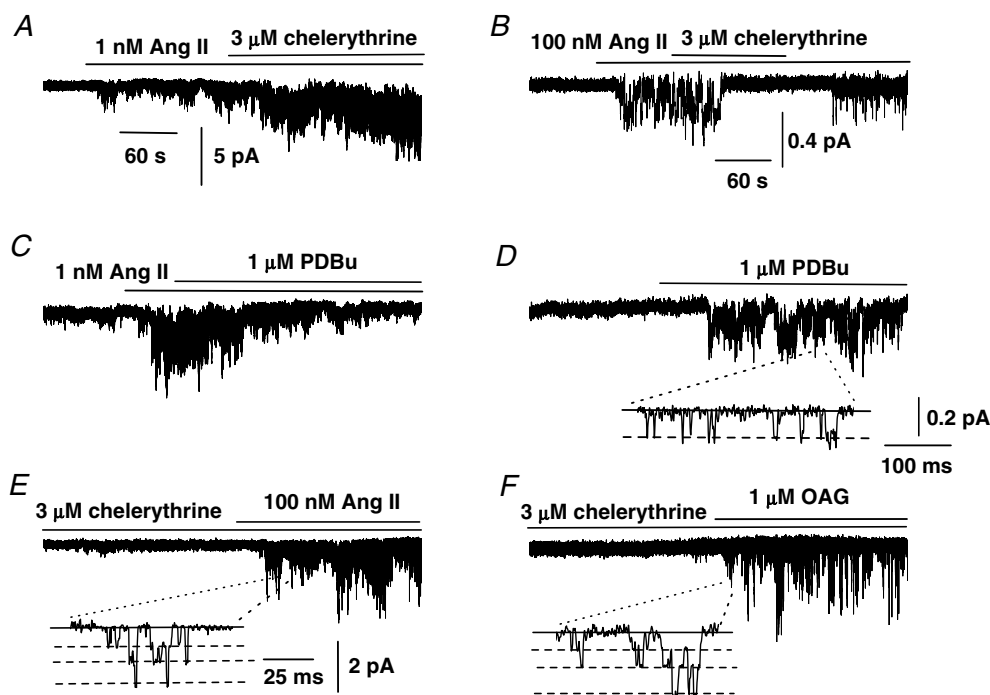


Figure 4. Effect of the protein kinase C (PKC) inhibitor chelerythrine and PKC activator phorbol-12, 13-dibutyrate (PDBu) on $I_{\text{cat}1}$ and $I_{\text{cat}2}$ in cell-attached patches

A, shows that 3 μM chelerythrine increased the activity of 1 nM Ang II-evoked $I_{\text{cat}1}$ at -50 mV. B, 3 μM chelerythrine inhibited activity of $I_{\text{cat}2}$ induced by 100 nM Ang II at -70 mV. C, shows that 1 μM PDBu reduced $I_{\text{cat}1}$ activity induced by 1 nM Ang II. D, bath application of 1 μM PDBu activated $I_{\text{cat}2}$ in a quiescent cell-attached patch at -70 mV. E and F, following preincubation with 3 μM chelerythrine, bath application of 100 nM Ang II (E) and 1 μM OAG (F) activated $I_{\text{cat}1}$ in cell-attached patches held at -50 mV.

we studied the effects of the cell-permeable Ca^{2+} chelator, BAPTA-AM, and the SR Ca^{2+} -ATPase inhibitor, cyclopiazonic acid (CPA), which are agents known to deplete intracellular Ca^{2+} stores.

Figure 5A and B shows that bath application of 50 μM BAPTA-AM to a quiescent cell-attached patch activated cation channel currents that had mean NP_o of 0.167 ± 0.074 ($n = 10$) and unitary amplitudes of about -0.2 pA at -70 mV. The mean pooled $I-V$ relationship of the BAPTA-AM-evoked channel currents had a slope conductance between -120 and -50 mV of 2 pS and an extrapolated E_r of $+18$ mV (Fig. 5C). In addition we carried out experiments using a Ca^{2+} free cell-attached pipette solution (see Methods) and in these patches bath application of 50 μM BAPTA-AM activated cation channel currents with a conductance of 7.3 pS and an E_r of -4 mV (Fig. 5C). Moreover, Fig. 5D shows that co-application of 3 μM chelerythrine inhibited channel activity evoked by BAPTA-AM and in six patches the mean NP_o value of BAPTA-AM-induced channel activity was significantly reduced by $85 \pm 6\%$ ($P < 0.05$).

In addition, bath application of CPA also evoked cation channel activity with a mean NP_o value of 0.266 ± 0.17

($n = 6$) and the mean pooled $I-V$ relationship of these CPA-activated channel currents had a conductance of 1.9 pS and an extrapolated E_r of $+21$ mV.

These data show that agents that are known to deplete intracellular Ca^{2+} stores activate channel currents with similar biophysical properties and activation mechanisms to Ang II-evoked I_{cat2} . It should also be noted that in all patches tested application of BAPTA-AM and CPA did not activate I_{cat1} .

Effect of anti-TRPC antibodies on Ang II-evoked I_{cat1} and I_{cat2} activity in inside-out patches

There is increasing evidence that members of the TRP family of channel proteins, and in particular the TRPC subfamily, form cation channels in smooth muscle (for review see Beech *et al.* 2004; Albert & Large, 2006). In a previous study we used anti-TRPC antibodies to show that TRPC3 channel proteins are involved in mediating constitutively active cation channel in rabbit ear artery myocytes (Albert *et al.* 2006). Therefore, we have used a similar method to investigate the role of TRPC proteins, in particular TRPC3, TRPC6 and TRPC7 proteins

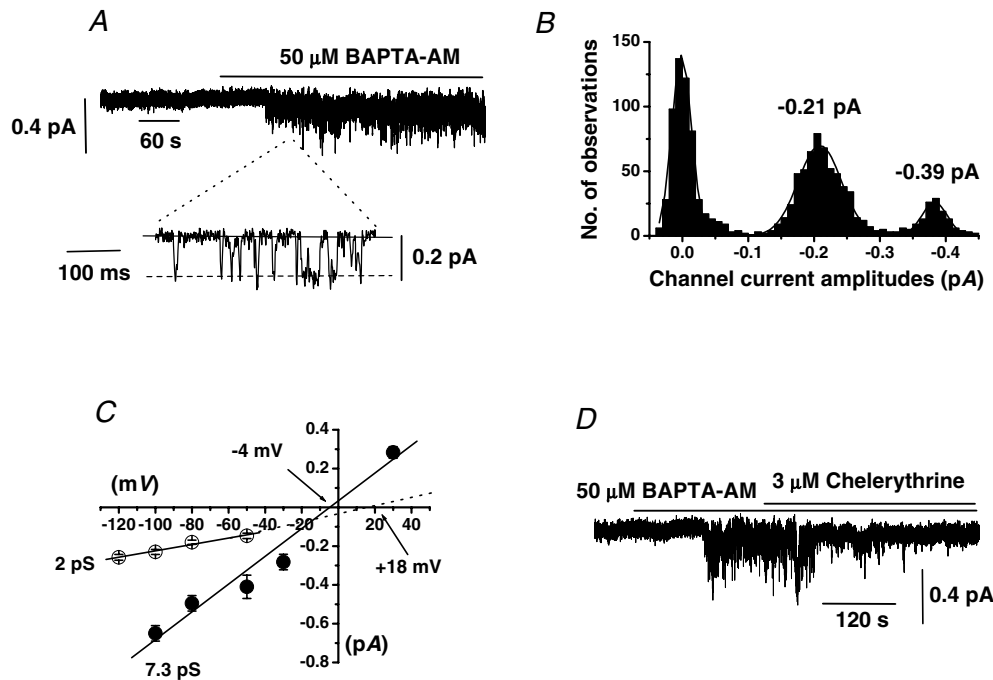


Figure 5. Effect of the cell-permeable Ca^{2+} chelator BAPTA-AM on cell-attached patches

A, bath application of 50 μM BAPTA-AM activated cation channel currents with a unitary amplitude of about -0.2 pA at -70 mV. B, amplitude histogram of BAPTA-AM-evoked channel currents shown in A which could be fitted with three Gaussians representing one closed and two unitary amplitude levels showing that this patch contained more than one channel. C, mean pooled $I-V$ relationships of BAPTA-AM-induced cation channel currents activated in 1.5 mM (○) or 0 [Ca^{2+}]_o (●). In 1.5 mM [Ca^{2+}]_o, BAPTA-AM channel currents had a unitary conductance of 2 pS with an extrapolated E_r of about $+18$ mV whereas in 0 [Ca^{2+}]_o these channels had a conductance of 7.3 pS and an E_r of about -4 mV. D, co-application of 3 μM chelerythrine inhibited channel currents evoked by BAPTA-AM at -70 mV.

which are activated by DAG via a PKC-independent mechanism (Trebak *et al.* 2003), and TRPC1 which has been proposed to mediate store-operated cation conductances in smooth muscle (Beech *et al.* 2004). In these experiments, I_{cat1} or I_{cat2} were activated in the cell-attached configuration by bath application of, respectively, 1 nM and 100 nM Ang II and then patches were excised into the inside-out configuration (see Methods for inside-out bathing solution). In this configuration, I_{cat1} and I_{cat2} were maintained for more than 10 min which allowed anti-TRPC antibodies to be applied to the cytoplasmic surface of the patches.

Figure 6A shows that bath application of anti-TRPC6sc antibodies at 1:200 dilution reversibly inhibited I_{cat1} activity induced by 1 nM Ang II in an inside-out patch held at -50 mV. Figure 6B shows the mean data from these experiments and illustrates that both anti-TRPC6sc and anti-TRPC6a antibodies significantly reduced Ang II-induced I_{cat1} activity by over 70%. Moreover, these data show that in the presence of their antigenic peptides the anti-TRPC6sc and anti-TRPC6a antibodies had no

effect on I_{cat1} activity (Fig. 6B). We also examined the effect of anti-TRPC1, anti-TRPC3 and anti-TRPC7 antibodies at 1:200 dilution on Ang II-induced I_{cat1} and Fig. 6B shows that these antibodies had no effect on I_{cat1} activity.

Figure 6C shows that bath application of anti-TRPC1a antibodies at 1:200 dilution reversibly inhibited I_{cat2} activity evoked by 100 nM Ang II and Fig. 6D shows that both anti-TRPC1a and anti-TRPC1sc antibodies inhibited the mean NP_o values of I_{cat2} activity by over 80%. In addition, Fig. 6D shows that Ang II-evoked I_{cat2} activity was unaffected by anti-TRPC1 antibodies preincubated with their antigenic peptides or by antibodies raised against TRPC3, TRPC6 and TRPC7 channel proteins.

These data suggest that TRPC6 and TRPC1 channel proteins are essential components of Ang II-evoked I_{cat1} and I_{cat2} channel proteins, respectively. The important observation that anti-TRPC6 antibodies do not block I_{cat2} activity and anti-TRPC1 antibodies do not affect I_{cat1} activity further indicates that these antibodies exhibit selectivity.

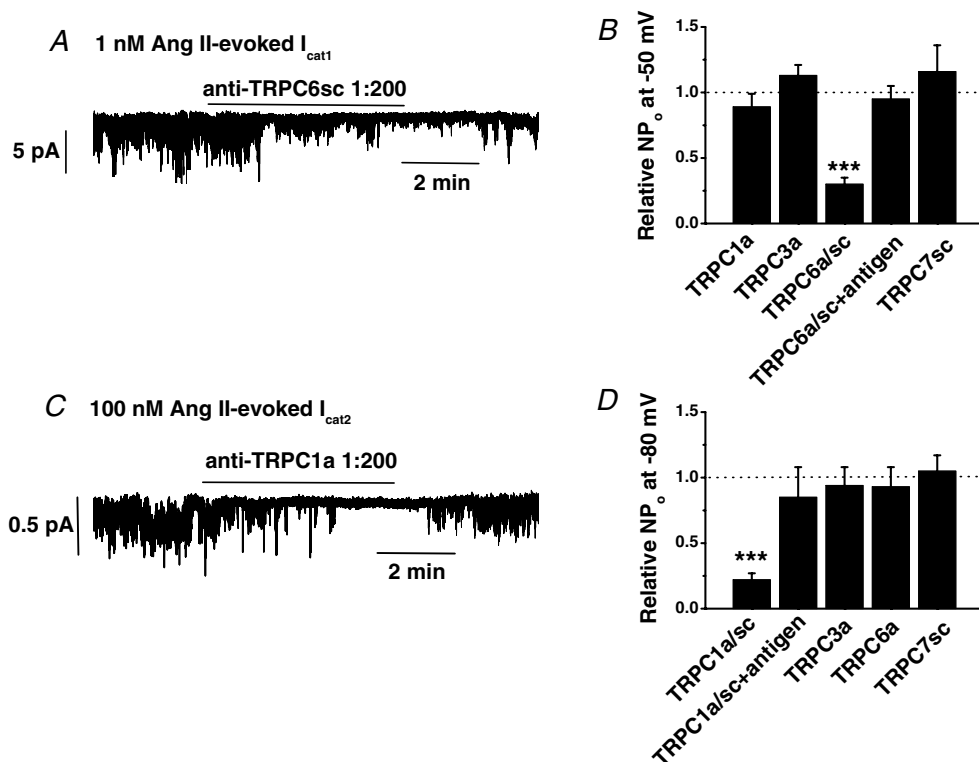


Figure 6. Effect of anti-TRPC antibodies on I_{cat1} and I_{cat2} in inside-out patches

A, bath application of anti-TRPC6sc antibodies at 1:200 dilution reversibly inhibited I_{cat1} stimulated by 1 nM Ang II at -50 mV. B, mean data showing that anti-TRPC6 antibodies significantly inhibited I_{cat1} activity whereas antibodies raised against TRPC1, C3 and C7 had no effect. Note that after preincubation with its antigenic peptide, anti-TRPC6 antibodies had no effect on I_{cat1} activity (** $P < 0.001$). C, bath application of anti-TRPC1a antibodies at 1:200 dilution reversibly inhibited I_{cat2} evoked by 100 nM Ang II at -70 mV. D, mean data showing the effect of anti-TRPC1, C3, C6 and C7 antibodies on I_{cat2} activity (** $P < 0.001$).

Effects of flufenamic acid and $0[Ca^{2+}]_o$ on Ang II-evoked I_{cat1} activity in outside-out patches

The previous data indicate that TRPC6 channel proteins are an important component of Ang II-evoked I_{cat1} and therefore we investigated the effect on I_{cat1} activity of flufenamic acid (FFA) and $0[Ca^{2+}]_o$ because they have been shown to be useful in discriminating TRPC6 channel currents from other TRPC channels, especially the closely related and DAG-activated channels proteins, TRPC3 and TRPC7 (see Table 1 in Albert *et al.* 2006).

Figure 7A shows that bath application of 1 nM Ang II to outside-out patches activated cation channel currents with a mean NP_o value of 0.780 ± 0.229 ($n = 14$) which in all patches tested exhibited three conductance states of 13, 27 and 47 pS and had similar E_r of about +5 mV (Fig. 7B). These values with outside-out recordings are similar to those data obtained with the cell-attached configuration. Figure 7Ca and 7D show that co-application of 100 μ M FFA increased the activity of I_{cat1} evoked by 1 nM Ang II whereas Fig. 7Cb and 7D illustrate that changing from 1.5 mM to $0[Ca^{2+}]_o$ reduced Ang II-evoked I_{cat1} activity. Moreover, $0[Ca^{2+}]_o$ had no effect on the three apparent

conductance states or E_r of Ang II-evoked I_{cat1} (data not shown) in contrast to the effects on I_{cat2} (see above).

The effects of FFA and $0[Ca^{2+}]_o$ on Ang II-evoked I_{cat1} activity are similar to their effects previously shown on expressed TRPC6 proteins (see Table 1 in Albert *et al.* 2006) and therefore these data provide further evidence that TRPC6 is an important component of I_{cat1} .

Expression of TRPC1 and TRPC6 channel proteins in rabbit mesenteric artery myocytes using immunocytochemical techniques

We investigated whether TRPC1 and TRPC6 proteins are present in mesenteric artery myocytes using immunocytochemical techniques combined with confocal microscopy, which enabled the expression and distribution of these TRPC proteins to be examined using the anti-TRPC6a and anti-TRPC1a antibodies which were shown earlier to block I_{cat1} and I_{cat2} activity (Fig. 6).

Figure 8A shows using anti-TRPC6a antibodies that rabbit mesenteric artery myocytes expressed TRPC6 proteins, and the mean data in Fig. 8C illustrate that

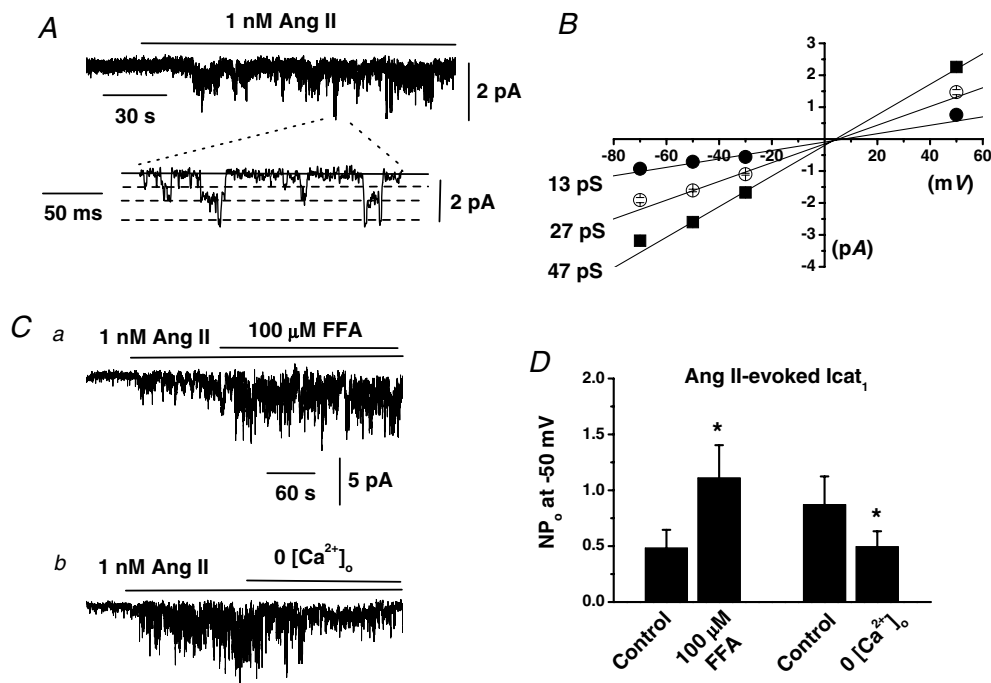


Figure 7. Effect of flufenamic acid (FFA) and $0[Ca^{2+}]_o$ on Ang II-evoked I_{cat1} in outside-out patches

A, bath application of 1 nM Ang II to an outside-out patch activated I_{cat1} at -50 mV. B, shows that the mean pooled I - V relationship of these channel currents had three conductance states of 13, 27 and 47 pS which all had an E_r of about +5 mV. C shows that bath application of 100 μ M FFA increased the activity of Ang II-induced I_{cat1} (a) and that changing from 1.5 mM to $0[Ca^{2+}]_o$ reduced activity of Ang II-evoked I_{cat1} (b). D, mean data showing the significant effects of FFA and $0[Ca^{2+}]_o$ on Ang II-induced I_{cat1} (* $P < 0.05$).

there was a significant 3-fold increase in fluorescence intensity for TRPC6 proteins close to the membrane (Region 1) compared to deeper in the cytoplasm (Region 2, $P < 0.001$). Figure 8B and C illustrate that mesenteric artery myocytes also expressed TRPC1 proteins using anti-TRPC1a antibodies but that the fluorescence intensity

of TRPC1 proteins was similar between Regions 1 and 2. Figure 8D shows that the fluorescence intensity of anti-TRPC1a and anti-TRPC6a staining were significantly reduced following preincubation with, respectively, the TRPC1a and TRPC6a antigenic peptides indicating selective binding to these TRPC proteins. Moreover, there

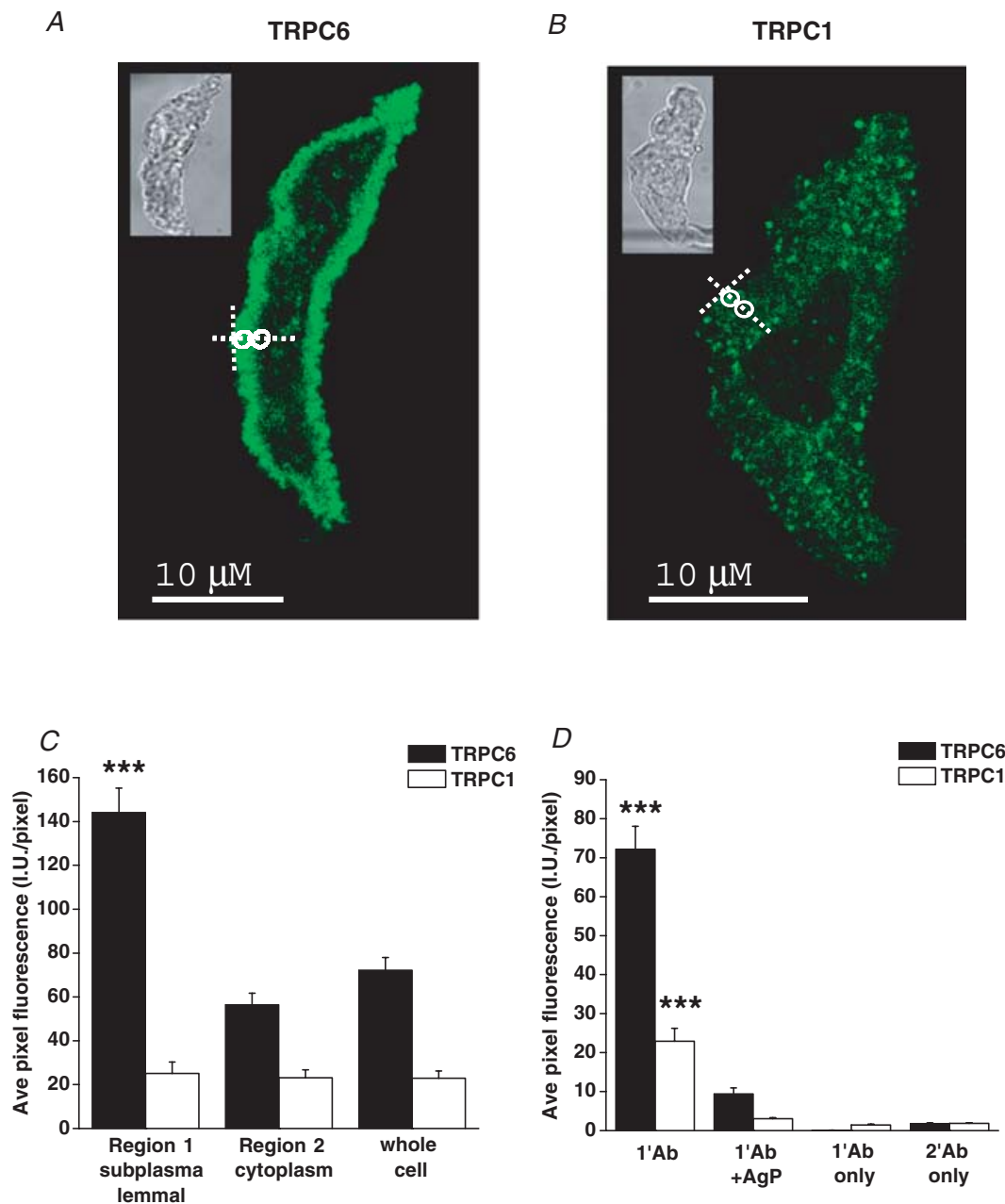


Figure 8. Immunocytochemical staining of rabbit mesenteric artery myocytes for TRPC1 and TRPC6 channel proteins

A and B, show single confocal plan fluorescence image of myocytes labelled with, respectively, anti-TRPC6a and anti-TRPC1a antibodies (1 : 50). Insets in A and B show transmitted light image of these myocytes. The white circles in A and B indicate Regions 1 and 2 used to analyse the distribution of fluorescence. C, mean data of distribution of fluorescence relating to binding of anti-TRPC6a and anti-TRPC1a antibodies. D, mean data illustrating intensity of fluorescence for anti-TRPC6a and anti-TRPC1a antibody binding in the presence of their antigenic peptides (1 : 25) and for binding of primary and secondary antibodies when incubated alone ($***P < 0.001$).

was no significant fluorescence signal in myocytes when primary or secondary antibodies were incubated alone.

Discussion

In the present study we have shown that in rabbit mesenteric artery smooth muscle cells Ang II activates two distinct cationic channels which differ in biophysical properties and gating mechanisms. The type of channel opened depends on the concentration of Ang II and both channels appear to be composed of TRPC proteins. The results demonstrate a novel and important principle that an agonist evokes two different TRPC channels with low concentrations predominantly activating TRPC6, whereas high concentrations inhibit TRPC6 and only channels with TRPC1 properties are stimulated.

Ang II stimulates two distinct cation channels

At low concentrations (1 nM), Ang II activated a cation channel (termed I_{cat1}) which contained three conductance states of approximately 15, 30 and 45 pS. These three conductance levels appear to be subconductance states of the same channel rather than different channels as the three states were observed in all patches tested with all activators used (cell-attached, inside-out and outside-out configurations), discrete transitions were observed between each state and all three states had similar E_r values of about 0 mV. However, the additive nature of the conductance levels means that we cannot exclude the possibility that the three states may represent multiple

openings of the same channel although this would require a high density of channel proteins at the plasmalemma for at least three channels to be present in every patch recorded. In contrast, relatively high concentrations (100 nM) of Ang II stimulated a cationic channel with a single conductance of about 2 pS (termed I_{cat2}) and an E_r of approximately +20 mV.

Removal of external Ca^{2+} ions had differential effects on I_{cat1} and I_{cat2} with $0[Ca^{2+}]_o$ increasing the unitary conductance of I_{cat2} from about 2 to 7 pS which was associated with a leftward shift in the E_r from approximately +20 to 0 mV, whereas $0[Ca^{2+}]_o$ had no effect on the apparent single-channel conductance or E_r of I_{cat1} although NP_o was decreased. It was not possible to obtain reversal of I_{cat2} at positive potentials and therefore we are cautious about the precision of the E_r value but nevertheless the overall data indicate that I_{cat2} has a greater permeability than I_{cat1} to Ca^{2+} ions.

Finally, PKC stimulation reduced I_{cat1} activity but appeared to be essential for evoking I_{cat2} . Therefore two biophysically different cation channels were activated by Ang II depending on the concentration used.

Transduction mechanism of I_{cat1} and I_{cat2}

The present work describes the signal transduction pathways involved in linking Ang II to activation of I_{cat1} and I_{cat2} ; these data are summarized in Fig. 9. Both I_{cat1} and I_{cat2} were blocked or substantially reduced by the AT_1 receptor antagonist losartan and the phosphoinositol-specific PLC inhibitor U73122. Moreover, the DAG analogue OAG, but

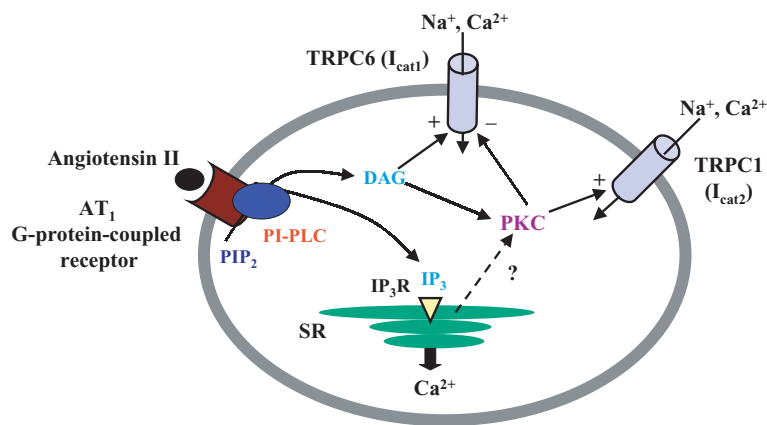


Figure 9. Schematic showing signalling pathways involved in Ang II activation and regulation of TRPC6 and TRPC1 channel proteins in mesenteric artery myocytes

Low concentrations of Ang II (1 nM) activate TRPC6 (and possibly TRPC1) but higher concentrations of Ang II (100 nM) stimulate only TRPC1. Activation of both channels involves stimulation of AT_1 receptors coupled to phosphoinositol-specific phospholipase C (PI-PLC) and diacylglycerol (DAG) production. TRPC6 is evoked by DAG via a protein kinase C (PKC)-independent gating mechanism whereas TRPC1 is activated via a PKC-dependent process which is also responsible for inhibiting TRPC6 at high Ang II concentrations. PIP₂, phosphatidylinositol 4,5-bisphosphate; IP₃, inositol 1,4,5-trisphosphate; SR, sarcoplasmic reticulum; IP₃R, inositol 1,4,5-trisphosphate receptor. +, activation; -, inhibition.

not IP₃, stimulated both channels. In addition the DAG lipase inhibitor RHC80267, which might be expected to elevate endogenous DAG levels in the membrane, also stimulated I_{cat1} and I_{cat2} providing further evidence for the involvement of DAG in the transduction pathway. However, the subsequent steps in the cascade differed in that activation of I_{cat1} was not mediated by PKC and in fact the data indicated that PKC inhibits stimulation of I_{cat1} (see below). In contrast, OAG- and Ang II-induced I_{cat2} were almost completely blocked by the PKC inhibitor chelerythrine and I_{cat2} channels were activated by phorbol esters in cell-attached patches. Thus it seems that the classical transduction mechanism involving AT₁ receptors, PLC and DAG production is implicated in stimulation of both Ang II-evoked channels but that I_{cat1} is mediated by DAG via a PKC-independent mechanism whereas I_{cat2} involves DAG stimulation of PKC and subsequent channel opening (Fig. 9).

PKC-mediated inhibition of I_{cat1}

There is substantial evidence that PKC inhibits I_{cat1} (see Fig. 9). First, the PKC inhibitor chelerythrine potentiated I_{cat1} evoked by 1 nM Ang II suggesting that there is a PKC-mediated inhibitory process opposing activation of the channel. Secondly, PDBu, which stimulates PKC, inhibited I_{cat1} induced by 1 nM Ang II. Moreover, 100 nM Ang II and OAG which only stimulated I_{cat2} in cell-attached patches in control conditions readily activated I_{cat1} in cells pretreated with the PKC inhibitor chelerythrine. It is tempting to speculate that PKC is important for the concentration-dependent effect of Ang II in evoking the two channels. With 1 nM Ang II it is possible that there is sufficient production of endogenous DAG to activate I_{cat1} via the PKC-independent mechanism but with 100 nM Ang II larger amounts of DAG are produced to cause more profound PKC stimulation which simultaneously inhibits I_{cat1} and activates I_{cat2} . Support for this hypothesis is provided by experiments with the DAG lipase inhibitor RHC80267 which initially activated I_{cat1} but after a few minutes I_{cat1} was inhibited and only I_{cat2} was observed. This pattern of events might be expected if RHC80267 caused a gradual build-up of endogenous DAG. Biochemical measurements were not made in the present work but previous studies have shown that in cultured rat aortic myocytes 100 nM Ang II stimulated maximal DAG production and moreover this concentration of agonist induced much greater DAG levels than with 1 nM Ang II (Griendling *et al.* 1986). In the same vascular preparation, Ang II has also been shown to activate PKC activity with a half-maximal effective concentration of about 1 nM (Lang & Vallotton, 1989). These data further support our hypothesis that the dose-dependent effects of Ang II on I_{cat1} and I_{cat2} are based

upon differences in the levels of agonist-induced DAG production and PKC stimulation.

An interesting observation was that in this preparation OAG activated I_{cat2} at very low concentrations with 1 nM OAG stimulating channel currents in several cells. The data above suggest that OAG activated I_{cat2} via PKC which also inhibits I_{cat1} , and therefore these results highlight the potency of PKC on these cation conductances in mesenteric artery myocytes. This observation may have relevance to other smooth muscle preparations in which cation currents evoked by G-protein-coupled receptor stimulation are markedly inhibited by the PLC inhibitor U73122 but bath applied OAG or intracellular application of IP₃ produce little or no response, for example in equine tracheal myocytes, (Wang & Kotlikoff, 2000) or guinea-pig small intestine (Zholos *et al.* 2004).

TRPC channels as molecular candidates for I_{cat1} and I_{cat2}

Application of anti-TRPC antibodies raised against putative intracellular epitopes of TRPC channel proteins to the cytoplasmic surface of inside-out patches provided evidence that different TRPC proteins are involved in forming the functioning ion channels underlying I_{cat1} and I_{cat2} . I_{cat1} evoked by 1 nM Ang II was markedly reduced by two different anti-TRPC6 antibodies and these inhibitory actions were completely blocked by preincubation with the antigenic peptides. In contrast, I_{cat1} was not affected by antibodies raised against members of the same sub-family (TRPC3 and TRPC7) or by anti-TRPC1 antibodies (two different antibodies raised against each TRPC protein). Moreover, immunocytochemical studies showed that TRPC6 proteins were expressed and preferentially localized to the plasma membrane, in keeping with a role as an ion channel utilized by extracellular agonists. With respect to antibody selectivity it is worth noting that in rabbit ear artery myocytes anti-TRPC3 antibodies produced marked inhibition of a constitutively active cation channel which was not affected by antibodies raised against other TRPC subtypes (Albert *et al.* 2006).

Further evidence that TRPC6 contributes to I_{cat1} is that FFA potentiated the channel activity whereas $0[Ca^{2+}]_o$ reduced the probability of channel opening. Also similar to expressed TRPC6 channels OAG stimulated I_{cat1} via a PKC-independent mechanism and PKC stimulation inhibited I_{cat1} (Inoue *et al.* 2001; Shi *et al.* 2004; and see Table 1 in Albert *et al.* 2006). Hence we conclude that TRPC6 is an important component of I_{cat1} .

In contrast I_{cat2} evoked by 100 nM Ang II was significantly inhibited by two different anti-TRPC1 antibodies but not affected by antibodies raised against TRPC3, C6 or C7. Moreover, the effects of the anti-TRPC1 antibodies were fully blocked by pretreatment with the

antigenic peptide. Also the immunocytochemistry studies showed TRPC1 staining inside myocytes but in this case we were not able to demonstrate preferential expression in the membrane. However the inhibition of I_{cat2} by application of anti-TRPC1 antibodies to excised inside-out patches indicates the presence of TRPC1 at, or close to, the membrane.

It has been reported that OAG activates TRPC1 (Lintschinger *et al.* 2000), supporting a role for TRPC1 in I_{cat2} , although in these experiments this was observed only in $0[Ca^{2+}]_o$, in contrast to the present work. Also several studies in vascular smooth muscle have implicated TRPC1 as a molecular constituent of SOCs (Xu & Beech, 2001; Sweeney *et al.* 2002; Brueggemann *et al.* 2006) and in the present work I_{cat2} was also evoked by agents that are known to deplete intracellular Ca^{2+} stores. Finally, it has been shown that TRPC1 may be activated by store depletion via a PKC-dependent mechanism which involves phosphorylation of TRPC1 (Ahmed *et al.* 2004). Therefore the combined data indicate that TRPC1 is a component of I_{cat2} but our work does not rule out the possibility that other TRPC proteins may contribute to the channel and further work is needed to elucidate the complete molecular composition of these channels. Recently it has also been shown that rat mesenteric artery smooth muscle cells contain TRPC1 and TRPC6 channel proteins using Western blotting and immunocytochemical techniques (Hill *et al.* 2006).

Comparison of I_{cat1} with other native TRPC currents

The above results provide strong evidence that TRPC6 is a molecular constituent of I_{cat1} but there are some notable differences compared to noradrenaline-evoked TRPC6 in rabbit portal vein myocytes (Inoue *et al.* 2001). First, in mesenteric artery I_{cat1} had conductance states of 15, 30 and 45 pS with the lowest value predominant in the presence of $1.5 \text{ mM } [Ca^{2+}]_o$. In portal vein there are only two states of about 13 and 23 pS and in the presence of $1.5 \text{ mM } [Ca^{2+}]_o$ most channels are in the 23 pS conformation (cf. present data with Albert & Large, 2001a, 2001b). Secondly, IP_3 potentiates OAG-evoked native TRPC6 in portal vein (Albert & Large, 2003) but not I_{cat1} in mesenteric artery myocytes (present work). It is evident that there are significant differences between TRPC6 in portal vein and mesenteric artery. It is interesting that expressed TRPC6 channels in HEK293 cells are also not potentiated by IP_3 (Shi *et al.* 2004; Estacion *et al.* 2004).

It is also worth noting that whereas U73122-sensitive PLC mediates noradrenaline- and Ang II-evoked TRPC6 currents in, respectively, portal vein (Helliwell & Large, 1997; Inoue *et al.* 2001) and mesenteric artery (present work), this pathway can have an inhibitory influence on constitutively active TRPC3 channels in rabbit ear artery

where phospholipase D is involved in generating DAG to activate TRPC3 channels (Albert & Large, 2004; Albert *et al.* 2005).

Is I_{cat2} stimulated in response to depletion of internal Ca^{2+} stores?

Biophysically similar channels to Ang II-evoked I_{cat2} , but not I_{cat1} , were stimulated by manipulations (addition of CPA or BAPTA-AM) which are known to release Ca^{2+} from intracellular stores. This raises the possibility that Ang II-evoked I_{cat2} is due to IP_3 -mediated release of Ca^{2+} from the SR (i.e. it is a SOC; Fig. 9). However, I_{cat2} was evoked by application of PDBu to inside-out patches (i.e. store-independent activation of the channel), and moreover BAPTA-AM and CPA may regulate I_{cat2} activity by altering cytosolic $[Ca^{2+}]$ which may affect various Ca^{2+} -dependent mechanisms involved in linking Ang II to opening of these channels. In portal vein myocytes, previous studies have also shown that noradrenaline-evoked SOCs were evoked by a store-independent but PKC-dependent mechanism (Albert & Large, 2002b) and that these 2 pS SOCs are stimulated by agents that inhibit protein kinase A (Liu *et al.* 2004), Ca^{2+} -dependent calmodulin kinase II (Albert *et al.* 2006) and calmodulin (Albert & Large, 2002a; Albert *et al.* 2006), and thus this channel is activated by mechanisms unrelated to store-depletion. Therefore it might be more accurate to term this channel a multiple-operated channel (MOC, Albert *et al.* 2006). Thus the results of the present work do not clearly show whether Ang II-evoked I_{cat2} is a consequence of release of Ca^{2+} from intracellular stores and further work is needed to test this hypothesis.

Conclusions

The results clearly show that Ang II evokes two distinct non-selective cation channels which cause depolarization and Ca^{2+} influx in rabbit mesenteric artery smooth muscle cells to produce vasoconstriction and increase total peripheral resistance and blood pressure. The data indicate that TRPC subunits are significant constituents of these channels and low concentrations of Ang II activate TRPC6, and possibly TRPC1, whereas high concentrations of Ang II preferentially stimulate TRPC1.

References

- Ahmed GU, Mehta D, Vogel S, Holinstat M, Paria BC, Tirupathi C & Malik AB (2004). Protein kinase $C\alpha$ phosphorylates transient receptor potential channel-1 (TRPC1) and regulates store-operated Ca^{2+} entry. Role in signalling increased endothelial permeability. *J Biol Chem* **279**, 20941–20949.

- Albert AP & Large WA (2001a). Comparison of spontaneous and noradrenaline-evoked non-selective cation channels in rabbit portal vein myocytes. *J Physiol* **530**, 457–468.
- Albert AP & Large WA (2001b). The effect of external divalent cations on spontaneous non-selective cation channel currents in rabbit portal vein myocytes. *J Physiol* **536**, 409–420.
- Albert AP & Large WA (2002a). A Ca^{2+} -permeable non-selective cation channel activated by depletion of internal Ca^{2+} stores in single rabbit portal vein myocytes. *J Physiol* **538**, 717–728.
- Albert AP & Large WA (2002b). Activation of store-operated channels by noradrenaline via protein kinase C in rabbit portal vein myocytes. *J Physiol* **544**, 113–125.
- Albert AP & Large WA (2003). Synergism between inositol phosphates and diacylglycerol on native TRPC6-like channels in rabbit portal vein myocytes. *J Physiol* **552**, 789–795.
- Albert AP & Large WA (2004). Inhibitory regulation of constitutive transient receptor potential-like cation channels in rabbit ear artery myocytes. *J Physiol* **560**, 169–180.
- Albert AP & Large WA (2006). Transduction pathways and gating mechanisms of native TRP-like channels in vascular myocytes. *J Physiol* **570**, 45–51.
- Albert AP, Piper AS & Large WA (2003). Properties of a constitutively active Ca^{2+} -permeable non-selective cation channel in rabbit ear artery myocytes. *J Physiol* **549**, 143–156.
- Albert AP, Piper AS & Large WA (2005). Role of phospholipase D and diacylglycerol in activating constitutive TRPC-like cation channels in rabbit ear artery myocytes. *J Physiol* **566**, 769–780.
- Albert AP, Pucovsky V, Prestwich SA & Large WA (2006). TRPC3 properties of a native constitutively active Ca^{2+} -permeable cation channel in rabbit ear artery myocytes. *J Physiol* **571**, 361–369.
- Beech DJ, Muraki K & Flemming R (2004). Non-selective cationic channels of smooth muscle and the mammalian homologues of *Drosophila* TRP. *J Physiol* **559**, 685–706.
- Brueggemann LI, Markun DR, Henderson KK, Cribbs LL & Byron KL (2006). Pharmacological and electrophysiological characterization of store-operated currents and capacitative Ca^{2+} entry in vascular smooth muscle cells. *J Pharmacol Exp Ther* **317**, 488–499.
- Clapham DE (2003). TRP channels as cellular sensors. *Nature* **426**, 517–524.
- Colquhoun D (1987). Practical analysis of single channel records. In *Microelectrode Techniques*, ed. Standen NB, Gray PTA & Whitaker MJ, pp. 83–104. The Company of Biologists, Cambridge.
- Estacion M, Li S, Sinkins WG, Gosling M, Bahra P, Poll C, Westwick J & Schilling WP (2004). Activation of human TRPC6 channels by receptor stimulation. *J Biol Chem* **279**, 22047–22056.
- Griendling KK, Rittenhouse SE, Brock TA, Ekstein LS, Gimbrone MA & Alexander RW (1986). Sustained diacylglycerol formation from inositol phospholipids in angiotensin II-stimulated vascular smooth muscle cells. *J Biol Chem* **261**, 5901–5906.
- Hamill OP, Marty A, Neher E, Sakmann B & Sigworth FJ (1981). Improved patch-clamp techniques for high-resolution current recording from cells and cell-free membrane patches. *Pflugers Arch* **391**, 85–100.
- Helliwell RM & Large WA (1997). Alpha 1-adrenoceptor activation of a non-selective cation current in rabbit portal vein by 1,2-diacyl-sn-glycerol. *J Physiol* **499**, 417–428.
- Hill AJ, Hinton JM, Cheng H, Gao Z, Bates DO, Hancox JC, Langton PD & James AF (2006). A TRPC-like non-selective cation current activated by $\alpha 1$ -adrenoceptors in rat mesenteric artery smooth muscle cells. *Cell Calcium* **40**, 29–40.
- Hughes AD & Bolton TB (1995). Action of angiotensin II, 5-hydroxytryptamine and adenosine triphosphate on ionic currents in single ear artery cells of the rabbit. *Br J Pharmacol* **116**, 2148–2154.
- Inoue R, Okada T, Onoue H, Harea Y, Shimizu S, Naitoh S, Ito Y & Mori Y (2001). The transient receptor potential homologue TRP6 is the essential component of vascular α -adrenoceptor-activated Ca^{2+} -permeable cation channel. *Circ Res* **88**, 325–337.
- Lang U & Vallotton MB (1989). Effects of angiotensin II and of phorbol ester on protein kinase C activity and on prostacyclin production in cultured rat aortic smooth muscle cells. *Biochem J* **259**, 477–484.
- Large WA (2002). Receptor-operated Ca^{2+} -permeable non-selective cation channels in vascular smooth muscle: a physiologic perspective. *J Cardiovasc Electrophysiol* **13**, 493–501.
- Lintschinger B, Balzer-Geldsetzer M, Baskaran T, Graier WF, Romanin C, Zhu MX & Groschner K (2000). Coassembly of Trp1 and Trp3 proteins generates diacylglycerol and Ca^{2+} -sensitive cation channels. *J Biol Chem* **275**, 27799–27805.
- Liu M, Large WA & Albert AP (2004). Stimulation of beta-adrenoceptors inhibits store-operated channel currents via a cAMP-dependent protein kinase mechanism in rabbit portal vein myocytes. *J Physiol* **562**, 395–406.
- Reading SA, Earley S, Waldon BJ, Welsh DG & Brayden JE (2005). TRPC3 mediates pyrimidine receptor-induced depolarisation of cerebral arteries. *J Physiol* **288**, H2055–H2061.
- Shi J, Mori E, Mori Y, Li J, Ito Y & Inoue R (2004). Multiple regulation by calcium of murine homologues of transient receptor potential proteins TRPC6 and TRPC7 expressed in HEK293 cells. *J Physiol* **561**, 415–432.
- Sweeney M Yu Y, Platoshyn O, Zhang S, McDaniel SS & Yuan JX (2002). Inhibition of endogenous TRP1 decreases capacitative Ca^{2+} entry and attenuates pulmonary artery smooth muscle cell proliferation. *Am J Physiol Lung Cell Mol Physiol* **283**, L144–L155.
- Touyz RM & Schiffrin EL (2000). Signal transduction mechanisms mediated the physiological and pathophysiological actions of angiotensin II in vascular smooth muscle cells. *Pharmacol Rev* **52**, 639–672.

- Trebak M, Vazquez G, Bird GJ & Putney JW (2003). The TRPC3/6/7 subfamily of cation channels. *Cell Calcium* **33**, 451–461.
- Wang YZ & Kotlikoff MI (2000). Signalling pathway for histamine activation of non-selective cation channels in equine tracheal myocytes. *J Physiol* **523**, 131–138.
- Xu S-Z & Beech DJ (2001). TrpC1 is a membrane-spanning subunit of store-operated Ca^{2+} channels in native vascular smooth muscle cells. *Circ Res* **88**, 84–87.

- Zholos AV, Tsytsyura YD, Gordienko DV, Tsvilovsky VV & Bolton TB (2004). Phospholipase C, but not InsP3 or DAG, -dependent activation of the muscarinic receptor-operated cation current in guinea-pig ileal smooth muscle cells. *Br J Pharmacol* **141**, 23–36.

Acknowledgements

This work was supported by The Wellcome Trust and British Heart Foundation.